

Supporting Information

Characterization of the dynamic growth of the nanobubble within the confined glass nanopore

Yong-Xu Hu, Yi-Lun Ying*, Rui Gao, Ru-Jia Yu, Yi-Tao Long*

¹ Key Laboratory for Advanced Materials & School of Chemistry and Molecular
Engineering,

East China University of Science and Technology, Shanghai 200237, P. R. China

Table of contents

Material -----	S-2
Preparation and characterization of the nanopore -----	S-2
Electrochemical recording and data analysis -----	S-3
Simulation of bubble radius – ionic current trace -----	S-4

1. Materials

All reagents were analytical grade, sodium phosphate monobasic (NaH_2PO_4 , 99%), sodium phosphate dibasic (Na_2HPO_4 , 99%) were purchased from Shanghai Lingfeng Chemical Reagent Co., Ltd. (Shanghai, China). NaBH_4 and ethanol ($\geq 99\%$) was obtained from Shanghai Guoyao Co., Ltd. (Shanghai, China). The tetrabutylammonium hexafluorophosphate (TBAPF_6) was purchase from Sigma-Aldrich (St. Louis, MO, U.S.A.). All solutions for analytical studies were prepared with ultrapure water (reaching a resistivity of $18.2 \text{ M}\Omega \text{ cm}$ at 25°C) obtained using a Milli-Q System (EMD Millipore, Billerica, MA, U.S.A.). A pair of platinum wire (0.5 mm, Alfa Aesar Co., Ward Hill, MA, U.S.A.) was used as the electrode.

2. Preparation and characterization of the nanopore

The 45 nm radius nanopore were fabricated by laser pulling of glass capillaries (O.D.=1.0 mm, I.D.=0.70 mm, length=7.5 cm, Sutter Instrument Co., Novato, CA, U.S.A.) using a P-2000 capillary puller (Sutter Instrument Co., Novato, CA, U.S.A.). The pulling parameter was shown as below: Heat 650, Fil 4, Vel 45, Del 170, Pul 205. The 150 nm radius nanopore was pulled by the following parameter: Heat 650, Fil 3, Vel 27, Del 170, Pul 205. The 22.5 nm radius nanopore were fabricated by laser pulling of glass capillaries with 0.5 mm interior diameter (O.D.=1.0 mm, I.D.=0.50 mm, length=7.5 cm, Sutter Instrument Co., Novato, CA, U.S.A.). The pulling parameter was followed a two-step process: Line 1, Heat 650, Fil 3, Vel 35, Del 145, Pul 75; Line 2, Heat 900, Fil 2, Vel 15, Del 128, Pul 200. The SEM characterization was performed by Zeiss Ultra Plus scanning electron microscope (Carl Zeiss, Oberkochen, Germany).

3. Electrochemical recording and data analysis

An Axopatch 700B low-noise amplifier (Molecular Devices, Sunnyvale, CA, USA) were used for current measurements. The amplifier's internal low-pass Bessel filter was set as 5 kHz. Data were acquired at a sampling rate of 100 kHz by using a DigiData 1550A converter and a PC running PClamp 10.6 (Axon Instruments, Forest City, CA, USA). The data analysis was performed using home-designed software (<http://ytlong.ecust.edu.cn/9148/list.htm>), the data plot was drawn by OriginLab 9.0 (OriginLab Corporation, Northampton, MA, USA) and the simulation was made by Comsol 5.3a (COMSOL Inc., Burlington, MA, USA)

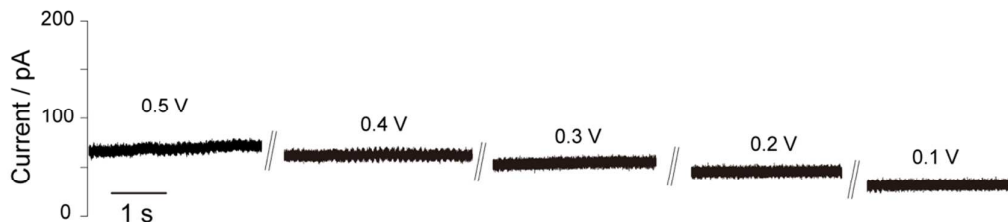


Figure S1. The current traces of nanopore backfilled with ethanol and immersed in the PBS solution. The ethanol solution is in the absence of NaBH_4 .

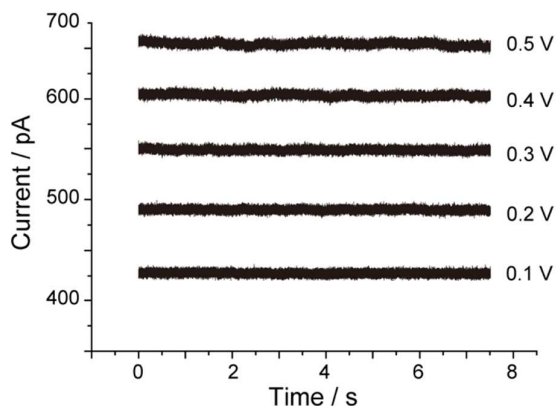


Figure S2. The current traces of nanopore immersed in the ethanol solution in the presence of 200 mM NaBH_4 . Both the external and internal solution were filled with ethanol solution.

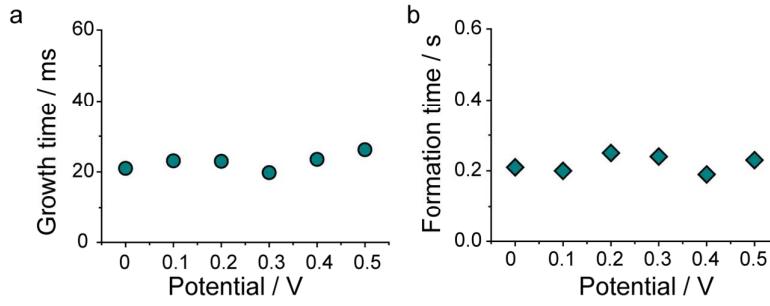


Figure S3. The variation of growth time (a) and formation time (b) at the applied potential increased from 0 mV to 500 mV.

4. Simulation of bubble radius – ionic current trace

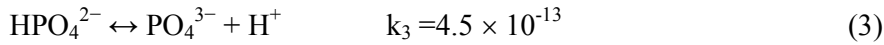
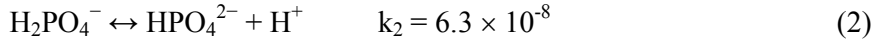
Coupled Poisson-Nernst-Planck (PNP) and Navier-Stokes (NS) equations were solved to model ionic current of nanopore with different bubble radius using a 2D symmetric model at room temperature of 298 K.¹ The geometry this model are set as $r = 45$ nm, $\theta = 5^\circ$. In our simulation, the surface charge density of pore wall is set as $\sigma_0 = -0.005$ C/m².² As the zeta potential of nanobubble in the ethanol solution is much lower than that in aqueous solution, we assume the enhanced current mainly comes from the BO_2^- group exposed in the PBS solution. To simplify the simulation, we only consider the PBS phase in our simulation.

The 2D axisymmetric geometry with a nanobubble set at the tip of nanopore are shown schematically in Figure S5. Detailed boundary condition is shown as Table S1. The dynamics of the ions in the channel is governed by the Poisson-Nernst-Planck (PNP) equations which relate surface charge with ionic fluxes and corresponding conductivity distribution within a glass nanopore. The Nernst-Planck equations describe the flux of ionic species, eq 1.

$$\mathbf{J}_i = -D_i \nabla c_i - \frac{z_i F}{RT} D_i c_i \nabla \Phi + c_i \mathbf{u} \quad (1)$$

Here, \mathbf{J}_i , D_i , c_i and z_i represent the flux, diffusion constant, concentration, and

charge of species i , respectively. Φ and \mathbf{u} are the local electric potential and fluid velocity; and F , R , and T are the Faraday constant, the gas constant, and the absolute temperature, respectively. J_i , c_i , Φ and \mathbf{u} are position-dependent quantities. To consider the equilibria of the $\text{H}_2\text{PO}_4^{2-}$ and HPO_4^{2-} in 10 mM PBS solution, we calculated the $[\text{Na}^+]$, $[\text{H}_2\text{PO}_4^{2-}]$, $[\text{HPO}_4^{2-}]$ and $[\text{PO}_4^{3-}]$ based on their ionization equilibrium as follows:



As the $k_3 \ll k_2$, the number of ionized of HPO_4^{2-} could be ignored in this simulation.

Therefore, the concentration of ions at equilibrium are shown as follows:

$c_{\text{Na}^+} = 0.0172 \text{ M}$, $c_{\text{HPO}_4^{2-}} = 0.0072 \text{ M}$, $c_{\text{H}_2\text{PO}_4^-} = 0.0028 \text{ M}$, $c_{\text{PO}_4^{3-}} = 1.3 \times 10^{-7} \text{ M}$.

The small concentration of PO_4^{3-} was ignored in our simulation.

The boundary condition in bulk solution (boundaries Φ and Ψ in Figure S5) is shown as follow:

$c_{\text{Na}^+} = 0.0172 \text{ M}$, $c_{\text{HPO}_4^{2-}} = 0.0072 \text{ M}$, $c_{\text{H}_2\text{PO}_4^-} = 0.0028 \text{ M}$,

The diffusion constant of these three species is set as $D_{\text{Na}^+} = 1.33 \times 10^{-9} \text{ m}^2/\text{s}$, $D_{\text{HPO}_4^{2-}} = 0.76 \times 10^{-9} \text{ m}^2/\text{s}$, $D_{\text{H}_2\text{PO}_4^-} = 0.96 \times 10^{-9} \text{ m}^2/\text{s}$.³

As neither species are transported into or out of the surface of glass (boundaries $\Psi, \Phi, \textcircled{4}, \textcircled{6}$, and Φ in Figure S5), there is no normal flux; the boundary condition is set as:

$$\mathbf{N} \cdot \mathbf{J}_i = 0$$

The relationship between the electric potential and ion concentration is described by Poisson equation, eq 4.

$$\nabla^2 \Phi = -\frac{F}{\epsilon} \sum_i z_i c_i \quad (4)$$

Where ϵ is the dielectric constant of the medium.

The flow distribution is given by the Navier-Stokes equation, eq 5, describing the pressure and electrical force driven flow.

$$\mathbf{u}\nabla\mathbf{u} = \frac{1}{\rho} (-\nabla p + \eta\nabla^2\mathbf{u} - F(\sum_i \sigma_i c_i)\nabla\Phi) \quad (5)$$

Here, ρ and η are the density and viscosity of the fluid, and p is the pressure.

Density ρ sets as $1 \times 10^{-3} \text{ kg/m}^3$ and viscosity η sets as $1 \times 10^{-3} \text{ Pa} \cdot \text{s}$.

To simulate the biphasic pulse in different sized glass nanopore, the nanobubble with different surface charge was introduced in to the tip of the nanopore (boundary ⑩ in Figure S5). The simulated bubble radius-ionic current curve corresponding to different surface charge of nanobubble are shown in Figure S4. The results reflect the maximum bubble radius nearly reaches to the radius of nanopore.

The finite element simulations were carried out with COMSOL Multiphysics 5.3a (COMSOL Inc., Burlington, MA, USA) operated on a Lenovo P500 workstation (Intel(R) Xeon(R) CPU E5-1620 v3@3.50GHz, 4core, 32GB RAM)

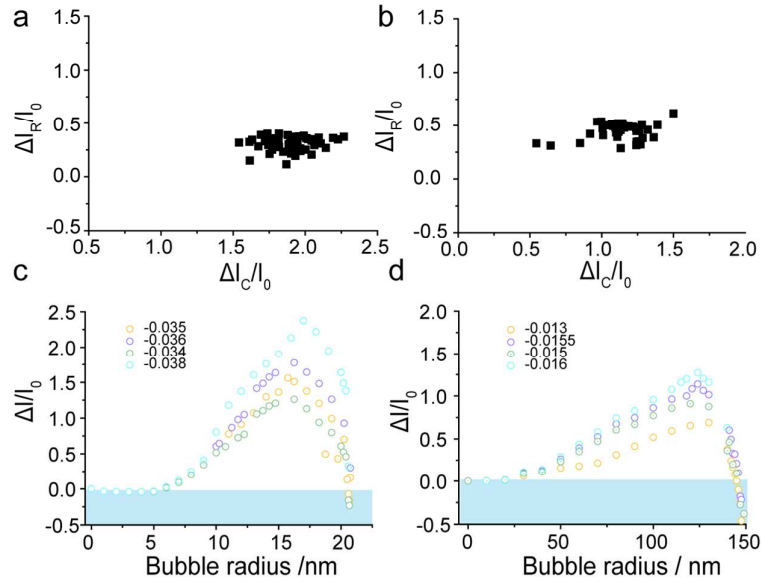


Figure S4. The scatter plot of $\Delta I_C/I_0$ versus $\Delta I_R/I_0$ corresponding to nanopore radius of 22.5 nm (a) and 150 nm (b). The simulated current-bubble radius trace for nanobubble with different surface charge density within the tip of glass nanopore of 22.5 nm (c) and 150 nm radius. (d) The blue rectangular marks the occurrence of resistant ionic current. Both the radius of nanobubble in 22.5 nm and 150 nm nanopore reach the value that approaching the nanopore radius.

Table S1. Boundary conditions for the numerical solution of Equations 1, 4 and 5 in the computation domain sketched in Figure S5 for the 2D axisymmetric geometry of the nanopore.

Surface	Nernst-Planck eq (eq 1)	Poisson eq (eq 4)	Navier-Stokes eq (eq 5)
⑧	$c_{Na^+}=17.2$ mM, $c_{HPO_4^{2-}}=7.2$ mM, $c_{H_2PO_4^-}=2.8$ mM	$V = 0$	$P = 0$ No viscous stress
②, ③, ④, ⑥, ⑦	No flux	No charge	No slip
⑤	No flux	$\sigma = -0.005$ C/m ²	No slip
①	$c_{Na^+}=17.2$ mM, $c_{HPO_4^{2-}}=7.2$ mM, $c_{H_2PO_4^-}=2.8$ mM	$V = 0.5$ V	$P = 0$ No viscous stress
⑨	Axial symmetry	Axial symmetry	Axial symmetry

3. Lide, D. R., Electronic Editions. *CRC Handbook of Chemistry and Physics*, 92nd Edition, Internet Version **2012**.